J Mater Sci (2012) 47:833–844
DOI 10.1007/s10853-011-5861-5

# Mechanism of synthesizing dense Si–SiC matrix C/C composites

**Shigeru Hanzawa**

Received: 18 May 2011 / Accepted: 8 August 2011 / Published online: 24 August 2011


**Abstract** The following technique is known to synthesize C/C (carbon fiber-reinforced carbon) composites. The organic matter in the preformed yarn (plastic straw covered yarn including bundles of long carbon fibers, carbon powder, and organic binder) is pyrolyzed at 500 °C and concurrently hot-pressed. Then, the carbon ingredient is graphitized in an atmosphere of nitrogen at 2000 °C. The authors used the above mentioned C/C composites as a starting material and developed a dense Si–SiC matrix C/C composites in which most long carbon fibers remain without reacting with Si which is infiltrated in argon at 1600 °C and 100 Pa. As a result, production of 1 × 2 m large size plates free from warps and cracks was attained in NGK Insulators, Ltd. This mechanism consists of three steps. First, a trunk-shaped Si–SiC matrix is synthesized between yarn and yarn. Then a trunk-shaped Si–SiC matrix extends a yarn by force. Only differential gap is made in a yarn surface. Finally, branch-shaped Si–SiC matrix is synthesized so that a trunk-shaped Si–SiC matrix leads to the yarn inside.

## Introduction

In 1950s, a high-density Si infiltrated SiC (Si–SiC) ceramics were developed by heating the compacted powder of SiC powder, carbon powder, and organic binder to 1500 °C at 0.5 mmHg in the presences of Si [1]. This ceramics has oxidation resistance, chemical corrosion resistance, and high temperature strength at the same level as hot-pressed SiC, along with high thermal conductivity, thermal shock resistance, impermeability, abrasion resistance, and other characteristics. These have been used widely in industrial fields including kiln furniture and semiconductor manufacturing process tube.

Light-weight and high-strength C/C (carbon fiber-reinforced carbon) composites were developed by heating the mix of molding products of carbon fibers and organic matter in an inert gas or mixture of methane and argon. This C/C composite is useful in severely abrasive, ablative, and corrosive environments. It has been used for brake disks for high speed cars and airplanes [2] and kiln furniture since 1970s.

After the above two materials were developed, the Si infiltrated C/C composites were developed in a vacuum at 1450–1550 °C to improve oxidation resistance and wear characteristics of the C/C composites [3]. However, Si infiltrated C/C composites having both characteristics of Si–SiC and C/C composites have not been put into practical use or industrialized. Therefore, to attain a Si infiltrated C/C composites, it was proposed by Fitzer that only porous carbon binder matrix should be converted to SiC selectively as almost all of the reinforced fibers are not corroded in the melted solution [4, 5].

Up to now, Chawla [6] and other researchers [7–12] have reported on the Si infiltrated C/C composites (hereinafter referred to as Si–SiC matrix C/C composites).

Nevertheless, the Si–SiC matrix C/C composites of the above mentioned microstructure causes the product to be warped and cracked and results in a low yield, which may have prevented the product from spreading. It can be understood from the fact that Si–SiC matrix C/C composites made with plane-weaved plate or carbon fibers sheet

S. Hanzawa (✉)
NGK Insulators, Ltd, Nagoya 467-8560, Japan
e-mail: hanzawa@ngk.co.jp

S. Hanzawa
Ceramics Research Laboratory, Nagoya Institute of Technology, Tajimi 507-0071, Japan

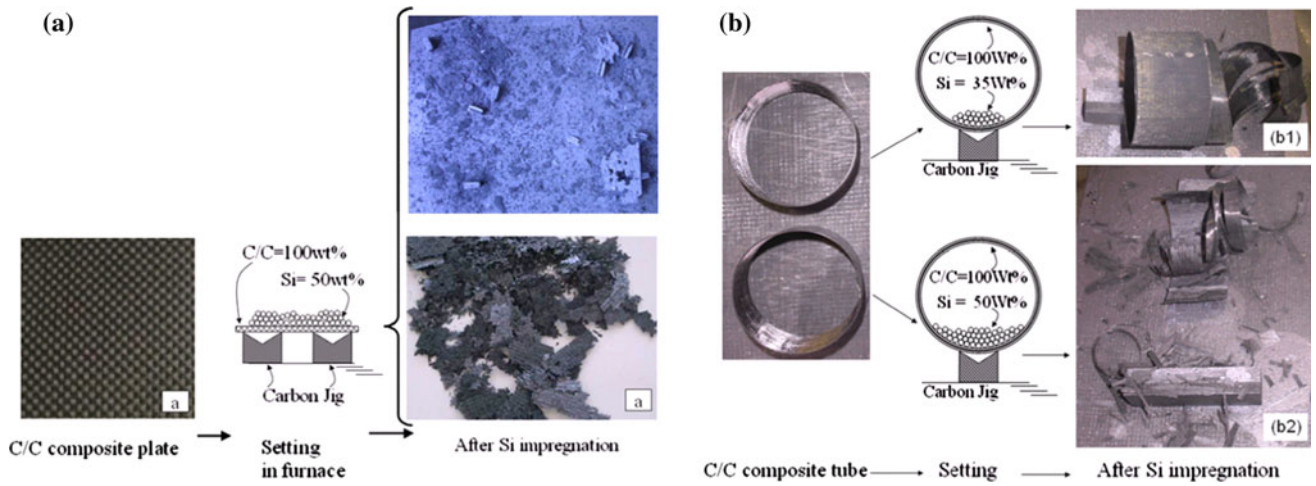


**Fig. 1** **a** Preliminary test result of Si infiltration with plane-weaved C/C composites. Case of scattering caused by Si infiltration. **b** Preliminary test result of Si infiltration with carbon fibers sheet-winded C/C composites. Case of scattering and deformation caused by Si infiltration

winded tube C/C composites made according to the known procedure [3], shown in Fig. 1a, b, causes scattering and deformation.

The mechanism synthesizing dense Si–SiC matrix C/C composites is reported for the purpose of showing the idea required in manufacturing industrial product of Si–SiC matrix C/C composites. First, the porous structure of the C/C composites as the starting material is considered. Next, the time-series state of making Si–SiC matrix by reacting carbons near the pores with Si to convert to SiC is observed. Finally, the behavior caused by the Si–SiC matrix synthesis is discussed.

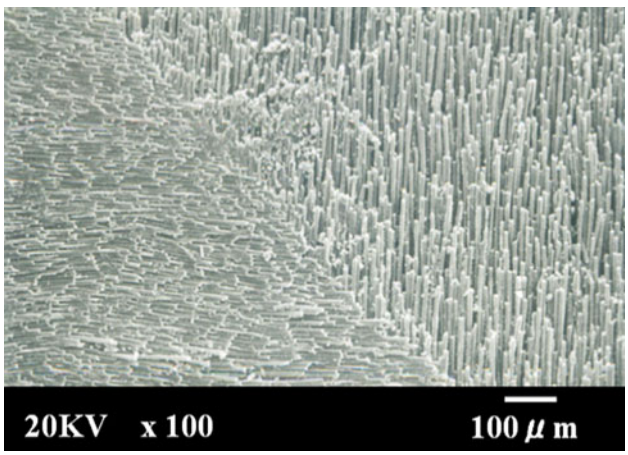


**Fig. 2** Microstructure (*sectional*) of plane-weaved C/C composites

## Experimental procedure

### Pore design of C/C composites

It can be said that the Si–SiC matrix structure in the C/C composites is an important element in designing Si–SiC matrix C/C composites with the original mechanical properties (i.e., high tensile strength). The yarn (low porosity area where each carbon fiber connects tightly in a bundle of fibers) is difficult to react with Si but the clearance between yarns is easy to react with Si. As the result, Si–SiC is synthesized mostly in the clearance between yarns. This fact may attain the structure proposed by Fitzer [4, 5] as mentioned in "Introduction". It means that the pore (porosity/pore diameter) of the C/C composites is a key element in designing materials.

The microstructure of the plane-weaved C/C composites used in the preliminary test (Fig. 1a) is shown in Fig. 2. The bundles of tightly connecting carbon fibers (yarn) contact vertically and horizontally. Each clearance between yarns is narrow, and each clearance between carbon fibers in the yarn is also similarly narrow. This plane of woven C/C composite has a structure that enables Si infiltration into the clearances "among yarns" and the clearances "among carbon fibers in yarns" at the almost same rate of speed. Infiltrated Si reacts with the carbon to synthesize SiC. Simultaneously, density change and volume change results in material scattering and deformation. Accordingly, the initial shape cannot be maintained.

In consideration of the above, the AC200-C/C composites synthesized according to the pre-pregnant sheet method [13] developed by ACROSS Co [14] was used as the starting material in this study. The AC200-C/C composites are synthesized according to the following procedure. The bundle of carbon fibers of 7 μm in diameter, carbon powder, and organic binder, bulk meso-phase of petroleum system (a volatile component is 17%), are

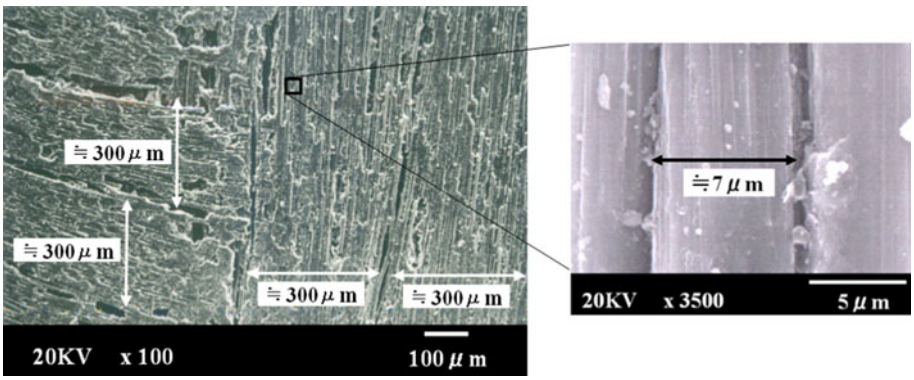


**Fig. 3** Microstructure (sectional) of AC200-C/C composites

covered with straw plastic tube to make preformed yarns. These preformed yarns are lined to make pre-pregnant sheets. The pre-pregnant sheet is cross laminated at 90° and hot-pressed at 1 MPa/500 °C to make a compact, which is put into a nitrogen atmosphere carbonize and graphitize furnace to heat to 1000 °C at 60 °C/h, then continued to 2000 °C at 300 °C/h and keep at the temperature for 30 min to make the plate type AC200-C/C composites.

During heating by hot press and graphitization, organic binder and plastic straw in the preformed yarn are pyrolyzed. A part of the pyrolized ingredients is gasified to form pores. As a result, the rest are graphitized to function as bonding materials for carbon fibers in the yarns and as yarn–yarn bonding materials of high porosity.

The microstructure of the AC200-C/C composites is shown in Fig. 3.

Figure 3 shows that the width of each yarn, in the AC200-C/C composites, is around 300 μm and that the diameter of the carbon fiber is around 7 μm. There are large/long pores among yarns vertically and horizontally in the similar directions as yarns. There are narrow/long pores (each diameter is smaller than that of carbon fibers) among carbon fibers in each yarn.

The relation between pore volume and pore diameter of the AC200-C/C composites is shown in Fig. 4. Pore volume of 7 μm (carbon fiber diameter) and more is approximately 70%, and pore volume of less than 7 μm is approximately 30%. The composites have bimodal pore distribution with 7 μm between pores.

The porosity of AC200-C/C composites is 16.05 vol% (Archimedes method, at 23 °C), the density is 1952.7 kg/m$^3$, and the absolute specific gravity is 1.9527 (at 23 °C). The values were determined with Micromeritics Gas Pycnometer (Accupyc1330-03) and the electronic balance (Mettler MT5).

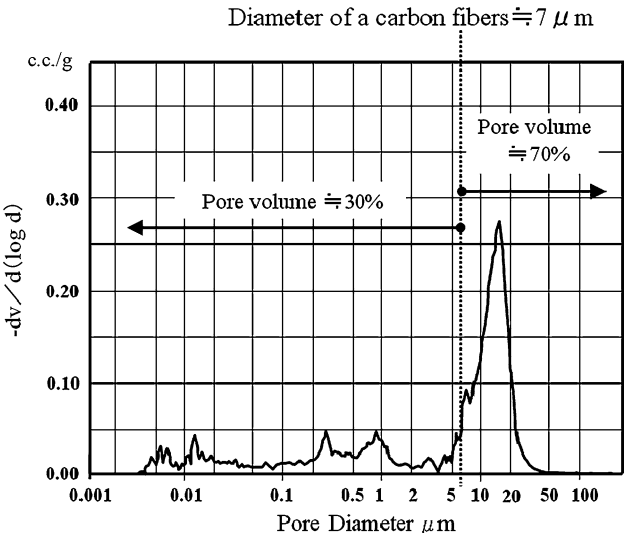


**Fig. 4** The relation between pore volumes and pore diameter of AC200-C/C

## Adjustment of Si volume

Mass-marketed ELKEM brand Si powder (2 mm or less in diameter, Si 99.5 wt%, $SiO_2$ 0.5 wt%) [15] was selected for this study. A fixed quantity of Si powder is loaded onto the AC200-C/C composites on the edged carbon jig (See Fig. 1a, b). The complete set is put into a furnace. The carbon jig between the furnace bottom base plate and the C/C composites prevents Si from contacting the furnace bottom base plate directly even if melted Si flows out. This is to prevent the furnace from being damaged [16]. The AC200-C/C composites with Si are heated at 100 Pa/Argon gas flow/1300 °C for 2 h to remove impurities in the $SiO_2$ in the Si powder and residual oxides in the C/C composites. The contact angle between Si and the other material should be small in the following heating (melted Si infiltration). In consideration of the fact that the contact angle between Si and $SiO_2$ (110° at 1450 °C, in 20 Torr with an Argon flow of 2 L/min [17]) is larger than the contact angle between Si and C (38° at 1430 °C, in Argon [18]), and it is important to remove $SiO_2$ and residual oxides. After removing the impurities of $SiO_2$ and oxides in AC200-C/C composites, Si is melted and infiltrated at the melting point (1410 °C)

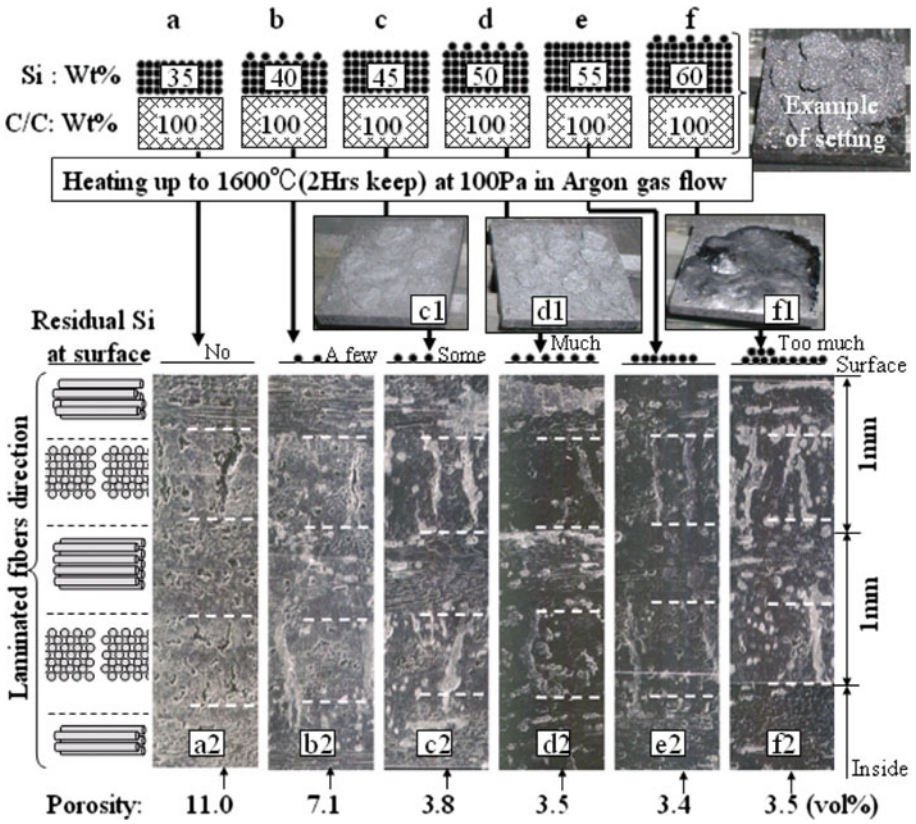


**Fig. 5** Si wt% infiltrated into AC200-C/C composites is determined by porosity

| Key | C/C (100wt%)+Si( a~f wt% ) | Heating → | Photo of surface | Cutting → | Photo of inside (Porosity ) |
|---|---|---|---|---|---|
| a | Ibid + a:35wt% | → | No photo | → | Photo a2 ( 11.0 vol% ) |
| b | Ibid + b:40wt% | → | No photo | → | Photo b2 ( 7.1 vol% ) |
| c | Ibid + c:35wt% | → | Photo c1 | → | Photo c2 ( 3.8 vol% ) |
| d | Ibid + d: 40wt% | → | Photo d1 | → | Photo d2 ( 3.5 vol% ) |
| e | Ibid + e: 55wt% | → | No photo | → | Photo e2 ( 3.4 vol% ) |
| f | Ibid + f: 55wt% | → | Photo f1 | → | Photo f2 ( 3.5 vol% ) |

and higher temperature to synthesize Si–SiC matrix C/C composites.

Figure 5 shows the procedure for determining optimum wt% of Si infiltrated into 100 wt% of AC200-C/C composites. 50 × 50 × 5 mm AC200-C/C composites (100 wt%) were used in this study. The quantity of Si added is changed from 35 to 60 wt% (six levels by 5 wt% steps). Those on the carbon jig are put into the furnace to determine optimum wt% of Si, at first heated to 1300 °C and then the temperature is kept for 2 h to remove $SiO_2$ and oxides, and then heated at 50 °C/h to 1600 °C (the temperature is kept for 2 h) and cooled. The heating atmosphere is an Argon gas flow of 1 L/min for 1 kg C/C composites to keep the pressure at 100 Pa [19]. Figure 5 shows the results of investigation of appearance/sectional photo/porosity of the six levels. As Si wt% increases, the pores among yarns are filled with Si and the porosity of AC200-C/C composites is reduced from 11.0 to 3.5%. Si infiltration into C/C composites stops at the porosity of 3.5%. The porosity is not reduced at more than 50 wt% of Si added. Accordingly, it can be said that the optimum Si wt% is 50 wt%. In consideration of evaporation loss of Si due to 100 Pa Argon atmosphere in large heating volume, a 50 wt% Si is determined as the standard in this study. Figure 5 also shows that dense Si–SiC matrix C/C composites of 3.5 vol% porosity can be obtained without scattering and deformation by infiltration or Si into the AC200-C/C composites regardless of Si added.

Figure 6d3 shows the microstructure of Si–SiC matrix C/C composites made with 50 wt% Si addition. Figure 6d4 shows the relation between the pore diameter and the pore volume of the material. In comparison between Fig. 3 (microstructure)/Fig. 4 (pore diameter and the volume) and Fig. 6d3 (microstructure)/Fig. 6d4 (pore diameter and the volume), the pores of 7 μm or more among yarns of the

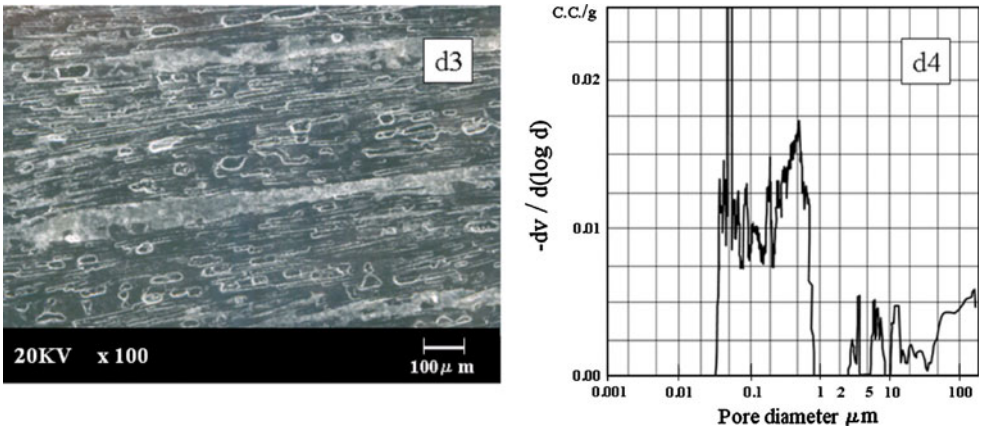


**Fig. 6** Microstructure of Si–SiC matrix C/C composites at Si = 50 wt% (**d3**) and the pore diameter/volume (**d4**)

Si–SiC matrix C/C composites obtained according in this procedure are filled with Si materials and pores of less than 7 μm still exist.

## Mechanism of synthesis and discussion

### Vol% of substance in Si–SiC matrix C/C composites

According to the Gern's calculation result [20] that pore capillary flow rate and Si infiltration height vary depending on pore sizes, and Si infiltration into the AC200-C/C composites is shown below in synthesizing Si–SiC matrix C/C composites.

At first, melted Si infiltrates into the porous carbon binder larger than 7 μm (many exist among yarns as shown in Fig. 3 and they are 70% of the total as shown in Fig. 4) and next melted Si infiltrates into pores of smaller than 7 μm (many exist among carbon fibers as shown in Fig. 3 and they are 30% of the total as shown in Fig. 4).

During the period of Si infiltration, pores in the C/C composites are filled up with Si to change the porosity. Simultaneously, Si reacts with C to make SiC. Accordingly, composition ratio of C/C, Si, and SiC in the produced Si–SiC matrix C/C composites cannot be readily determined. However, it can be estimated that there is a relationship between the content of C reacting with Si to synthesize SiC and the remaining properties of the C/C composites before Si infiltration. The porosity of AC200-C/C composites before Si infiltration is 16.05%, and the porosity of Si–SiC matrix C/C composites after Si infiltration is 3.5%. Figure 7 shows the results of calculation of the relative relation in volumes among C/C, SiC, and Si in Si–SiC matrix C/C composites with the parameter of SiC synthesized by the reaction of Si with C.

Figure 7 shows the case of synthesis of Si–SiC matrix C/C composites where Si does not react with C. 17 wt% Si infiltrates into 100 wt% AC200-C/C composites. C/C (carbon):Si:SiC:Pore in vol% = 85:11.5:0:3.5.

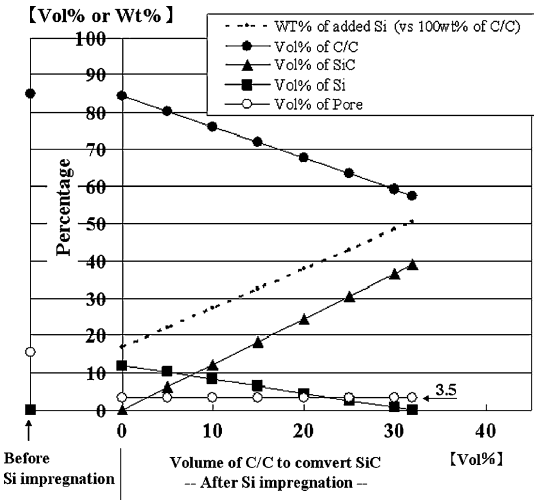


**Fig. 7** Relation between vol% of C/C·SiC·Si in Si–SiC matrix C/C composites (porosity 3.5%) and volume converted from C/C to SiC. Premise of specific density: C/C:Si:SiC = 1.9527:2.33:3.15, Range: No volume expansion in conversion from C/C to SiC

Figure 7 also shows the case of synthesis of Si–SiC matrix C/C composites where Si reacts with C fully. 50.5 wt% Si infiltrates into 100 wt% AC200-C/C composites. C/C (carbon):Si:SiC:Pore in vol% = 58:0:38.5:3.5.

The analysis result of chemical composition of Si–SiC matrix C/C composites in this study (shown in Fig. 6) and the chemical composition percentages according to Fig. 7 are shown in Table 1. As reviewed in "Adjustment of Si volume", infiltrated Si in this study is 50 wt%, which has enough residual Si at surface. Though it is needed to exclude Si wt% in Fig. 7, C/C (carbon):Si:SiC:Pore at *X*-axis 18 vol% (C/C volume converting to SiC), this agrees with the actual chemical analysis. Accordingly, this calculation is valid.

Targeted Si–SiC matrix C/C composites should include yarns of carbon fibers (which do not react with Si) and should have a 3D-network structure with Si–SiC matrix

**Table 1** Chemical composition of Si–SiC matrix C/C composites

| Material | Chemical analysis for Fig. 6d3 material | | Calculation *X*-vol% C/C convert to SiC at $X = 18$ (see Fig. 7) |
|---|---|---|---|
| | Vol% | Wt% | |
| Free-Si | 4.1 | (4.47) | 5 |
| Free-C | 71.8 | (65.52) | 70 |
| SiC | 20.6 | (29.45) | 21 |
| Porosity | 3.5 | | 3.5 |
| Total O | | (0.23) | |
| Total Si | | (25.30) | |
| Total C | | (74.74) | |

Chemical analysis by X-ray fluorescence performed in NGK Insulators, Ltd

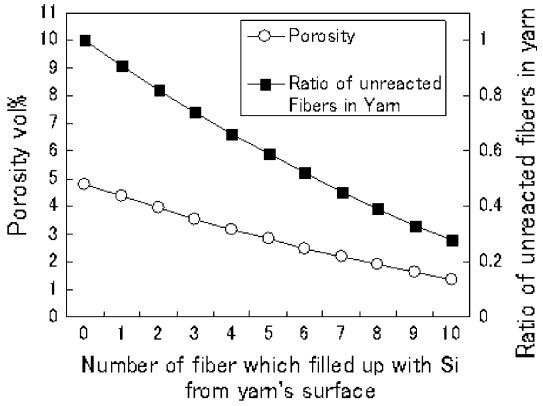


**Fig. 8** "Number of carbon fibers filled up with Si from the surface of the yarn" versus "Si–SiC matrix C/C composites pore vol% and ratio of un-reacted carbon fibers in Yarn"

among yarns where only the surfaces of yarns react with Si. Therefore, this is also considered in this study. The width of the yarn in the C/C composites in this study is approximately 300 μm (Fig. 3). If the section of the yarn is assumed to be square, a side of the yarn section holds 42.85 carbon fibers of 7 μm. Supposing that three carbon fibers from the yarn surface of 300 μm in width are filled up with Si–SiC, C/C composites of 16.05 vol% porosity is synthesized into Si–SiC matrix C/C composites of 3.55 vol% porosity from the following calculation (I) taking into consideration residual porosity and volume change from C to SiC in the same way as the calculation in Fig. 7, which agrees with chemical analysis.

$$3.55\ \text{vol}\% = 16.05\ \text{vol}\% \times 0.3 \times 0.74 \quad \text{(I)}$$

Here, the ratio of un-reacted fibers in yarn is 0.74 ($=258^2/300^2$), and the porosity of AC200-C/C composites is 16.05 vol%. The ratio of AC200-C/C composites pore of 7 μm or less is 0.3 (from Fig. 4). The width of yarn before Si infiltration is 300 μm (from Fig. 3). The width of un-reacted yarn is 258 μm (II).

$$258\,\mu\text{m} = (300\,\mu\text{m} - \text{yarn}/7\,\mu\text{m} - \text{fiber}) - (2\ \text{sides} \times 3\ \text{fibers}) \times 7\,\mu\text{m} \quad \text{(II)}$$

In supposing that *X*-pieces of carbon fibers from the surface of the yarn of 300 μm in width are filled up with Si, the relation of the number of carbon fibers filled up with Si and the Si–Si C matrix C/C composites porosity was calculated. Simultaneously, the ratio of un-reacted carbon fibers in yarn was estimated. The result is shown in Fig. 8.

In Fig. 8, it is estimated that Si–SiC matrix C/C composites of 3.5 vol% porosity has a microstructure, where 0.75 (75 vol%) carbon fibers do not react with Si, at synthesis of AC200-C/C composites. This may be the ideal microstructure proposed by Fitzer [4, 5].

## Effect of temperature on synthesis of dense Si–SiC matrix C/C composites

To study the effect of temperature on the synthesis of Si–SiC matrix C/C composites, three samples (T1, T2, and T3) were prepared as follows: Sample T1: 5 × 5 × 50-mm plate AC200-C/C composites with Si (weight ratio of Si:C/C composites is 50:100) was put into a furnace to heat to 1200 °C at 200 °C/h, then continued to heat to 1375 °C at 50 °C/h and keep at that temperature for 2 h. Sample T2: Similar to Sample T1, continued to heat to 1480 °C at 50 °C/h and kept for 2 h. Sample T3: Similar to Sample T1 and Sample T2, continued to heat to 1600 °C at 50 °C/h and kept for 2 h. The pressure was controlled to 100 Pa in the whole range of heating temperature. The atmosphere is Argon at 1 L/min for 1 kg of C/C composites. Photos of microstructures of the sectional surfaces of samples T1, T2, and T3 together with distribution of C concentration and Si concentration are shown in Fig. 9. The porosity of each sample is also shown in the figure. The surface of each sample of 5 mm in thickness was cut by 1 mm to determine the porosity by the Archimedes Method. Figure 10 shows the result of X-ray diffraction analysis of each sample for determining bulk density/porosity.

Sample T1 was obtained by heating at 1375 °C, which is lower than the Si melting point (1410 °C). There are no differences in microstructure and porosity between the sample and AC200-C/C composites before heat treatment. The distribution of Si concentration shows Si traced on the surface of AC200-C/C composites and the surfaces of pores among yarns. (Hereinafter the state of Sample T1 is referred to as "First Step".)

Sample T2 was heated at 1480 °C, which is 70 °C higher than the Si melting point (1410 °C). Large pores among the yarns in AC200-C/C composites are filled up

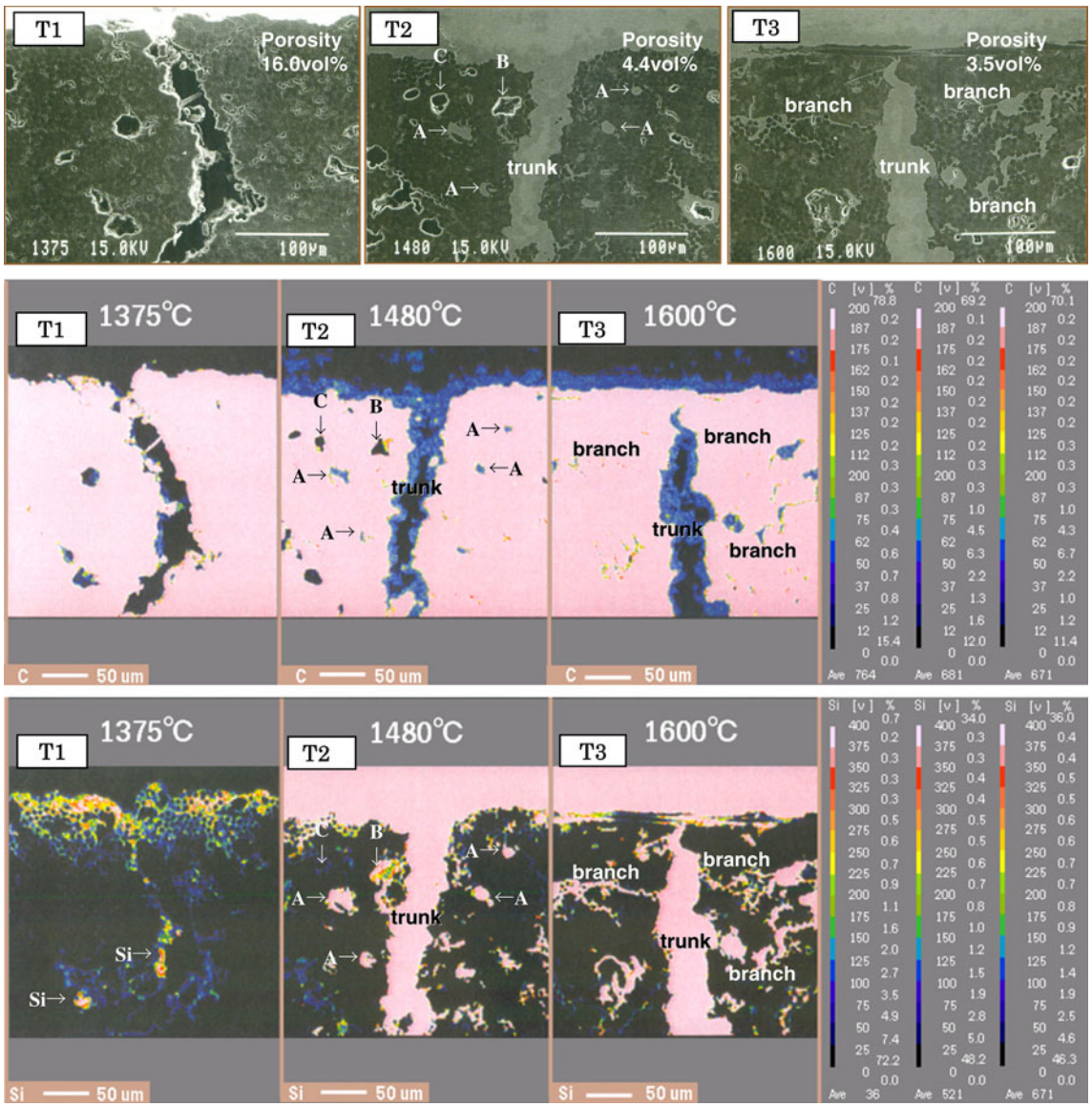


**Fig. 9** Photos of microstructure of Si–SiC matrix synthesized in AC200-C/C composites and Si concentration distribution image. T1 heat treated at 1375 °C "First Step", T2 heat treated at 1480 °C "Second Step", and T3 heat treated at 1600 °C "Third Step"

with Si and the porosity decreases to 4.4 vol%. However, some pores of 10 μm in diameter in yarns are filled up with Si (A), some are not completely filled up with Si though infiltrated (B), and Si does not infiltrate into some pores (C). The X-ray diffraction analysis in Fig. 10 shows that a part of infiltrated Si reacts with C to convert to SiC for synthesis of Si–SiC matrix. (Hereinafter, the state of Sample T2 is referred to as "Second Step".)

Sample T3 was heated at 1600 °C, which is 190 °C higher than the Si melting point (1410 °C). Si infiltrates into yarn pores of 10 μm in diameter in AC200-C/C composites and the porosity decreases to 3.5% to densify the material. Si is traced from the part filled up with Si among the trunk yarns to the branched pores of 10 μm in diameter in yarn. The infiltrated Si connects between the inside and the outside of the yarn to function as a path to fill up the pores of 10 μm in yarn with Si. Compared to the "Second Step", more Si reacts with C to convert to SiC for further synthesis of Si–SiC matrix. (Hereinafter, the state of Sample T3 is referred to as "Third Step".)

## First Step of Si–SiC matrix C/C composites synthesis

The "First Step" of the synthesis shown in Figs. 9 and 10 is the state that the carbon AC200-C/C composites and Si including 0.5 wt% of $SiO_2$ are heat treated at 1375 °C (70 °C lower than the Si melting point 1410 °C) for 2 h in 100 Pa Argon gas flow. A small quantity of SiC is traced in

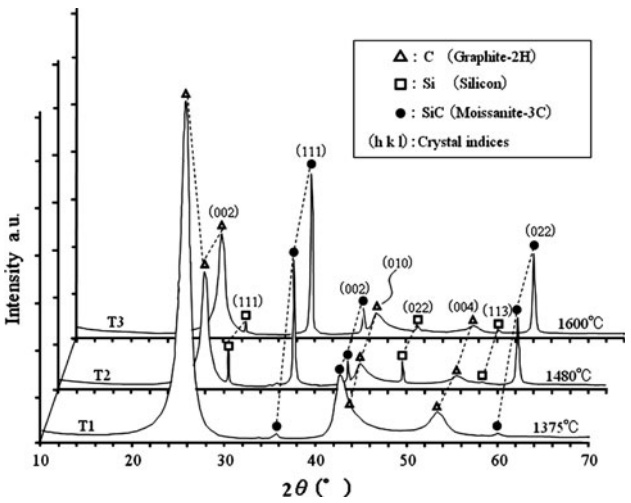


**Fig. 10** Crystal change at synthesis of Si–SiC matrix in AC200-C/C composites. T1 heat treated at 1375 °C, T2 heat treated at 1480 °C, and T3 heat treated at 1600 °C

the C/C composites as mentioned in "Effect of temperature on synthesis of dense Si–SiC matrix C/C composites".

Vapors (Si, SiO, $SiO_2$, CO, and $O_2$) react with carbons in C/C composites during heat treatment at 1375 °C for 2 h to synthesize the small quantity of SiC. From the thermodynamic data of these vapors [21] and the reaction of (1), (2), (3), (4), and (5), the relation between partial pressures of Si, SiO, and $SiO_2$ [22] at oxygen pressure of 100 Pa (same as atmospheric gas pressure) and temperature were calculated (Fig. 11, calculation method and results were taken from author's report [23]).

Equations of SiC, Si, SiO, $SiO_2$, CO, and $O_2$

$$SiC(s) + 3/2O_2(g) = SiO_2(s) + CO(g) + \Delta G1 \quad (1)$$

$$SiC(s) + O_2(g) = SiO(g) + CO(g) + \Delta G2 \quad (2)$$

$$SiO_2(s) = Si(g) + O_2(g) + \Delta G3 \quad (3)$$

$$2SiO_2(s) = 2SiO(g) + O_2(g) + \Delta G4 \quad (4)$$

$$SiO_2(s) = SiO_2(g) + \Delta G5 \quad (5)$$

Si vapor partial pressure is 1E−23 Pa at 1375 °C (1648 K). Each pressure of SiO and $SiO_2$ is 1E−10 Pa, which is low. It means that SiC is synthesized with such low-pressure Si vapors. The Patent Material [24] states that 1920–2080 °C is required to cover the carbon surface with SiC using Si and Si gas. Pore size and length, Si vapor diffusion rate, and SiC synthesis speed have not yet been investigated. However, the gas including Si moves to the carbon surface even at low temperature/low pressure to synthesize SiC and covers the yarn surface of the C/C composites with SiC thick film as time passes.

## Second Step and Third Step of Si–SiC matrix C/C composites synthesis

The synthesis of Si–SiC matrix C/C composites is completed in "Second Step" and "Third Step" after "First Step" stated in "First Step of Si–SiC matrix C/C composites synthesis". At "Second Step", melted Si infiltrates among yarns and infiltrates into the inside of yarn incompletely. However, the remaining pores of 10 μm in diameter in yarn at "Second Step" are filled up with Si and most of the pores disappear at "Third Step". Gern [20] indicated that Si infiltrates into pores of several μm in carbon fibers and calculated the height of Si infiltration into 5-μm pores of 0.1 m at 100 s. In our study, most of 10 μm pores in yarn are not filled up with Si at "Second Step". There may

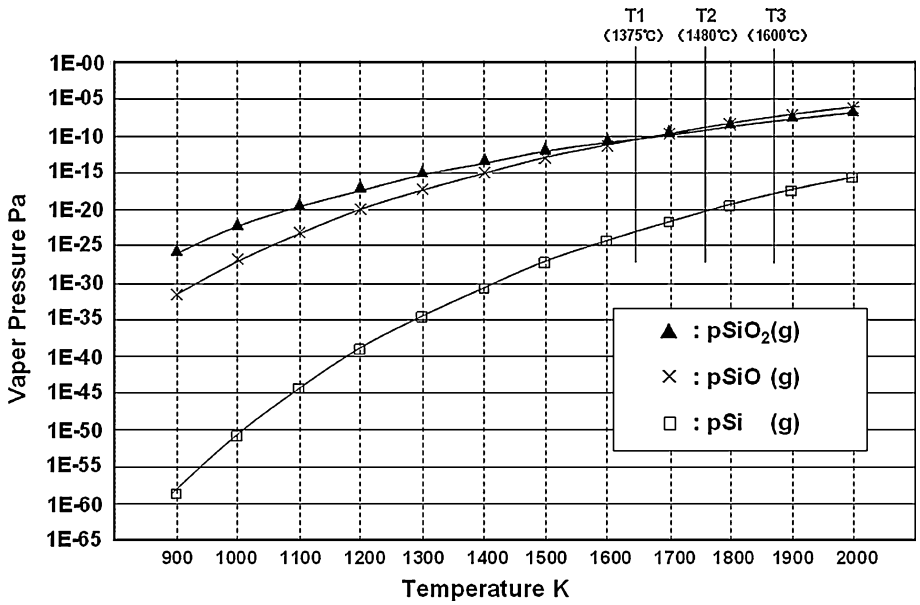


**Fig. 11** Relation between vapor pressures of Si, SiO, and $SiO_2$ at oxygen partial pressure of 100 Pa and temperature (Calculation method and results were taken from author's article [23])

be some causes for preventing Si from infiltrating. One of the causes is the very small clearances between carbon fibers in yarn. In addition, SiC films synthesized in vapors at "First Step" prevent Si infiltrated into large pores among yarns from infiltrating into the yarn inside. Simultaneously, thick SiC films are synthesized on the yarn surface at "Second Step". Accordingly, it may be estimated that Si infiltration into 10 μm pores in yarn is prevented. As the result, the state of "Second Step" of insufficient densification (Porosity 4.4%) may be caused. Next, "Third Step" is discussed, where Si infiltrates into 10 μm pores in yarn for densification after "Second Step" when Si infiltration stops. Figure 12 shows a photo of the microstructure of the area where yarn bonds with Si–SiC matrix. It is the enlarged photo of the area in the upper center of the photo of Sample T3 "Third Step" that is shown in Fig. 9. Figure 13 shows the microstructure of the area in the center in Fig. 12 (SEM), the result of Auger Analysis (AES) in Area 1 to Area 4 and the distribution of C concentration and Si concentration in the SEM area. In Figs. 12 and 13 (Area 2 and Area 3 are the areas containing Si and C), the trunk structure where the yarn surface is covered with 15–20 μm Si–SiC thick film and the branch structure of Si–SiC of 1 μm in width from the outside film of the trunk to the yarn inside can be observed. The outside Si–SiC film (15–20 μm in thickness) of the trunk structure is the synthesized SiC of 15–20 μm after 2-3 carbon fibers (7 μm in diameter) on the surface of the yarn are converted to Si–SiC. The number of carbon fibers changed to Si–SiC agrees with the reaction quantity stated in "Vol% of substance in Si–SiC matrix C/C composites" (Fig. 8).

## Trigger for the Third Step of Si–SiC matrix C/C composites synthesis

A trigger is required to go from "Second Step" to "Third Step" where Si–SiC matrix forms the branch structure Si–SiC growing from the trunk structure stated in "Second Step and Third Step of Si–SiC matrix C/C composites synthesis". This trigger is a crack from the trunk Si–SiC to the inside of the yarn which does not react with Si because (i) change in size (volume expansion) at synthesis of trunk Si–SiC structure contacting yarn causes strain in the yarn which does not react with Si and (ii) the tensile stress due to strain is higher than the tensile strength. Accordingly, Si in the trunk Si–SiC infiltrates through the trigger (crack) to synthesize dense Si–SiC matrix C/C composites of trunk Si–SiC, branch Si–SiC, and yarns not reacted.

At first, the above size change and strain (i) is stated. As discussed in "Second Step and Third Step of Si–SiC matrix C/C composites synthesis", 2-3 carbon fibers are converted to SiC and connect with the trunk Si–SiC on the surface of the yarn. In the area of 2-3 carbon fibers converted to SiC, the unit volume and the size of the initial carbon fiber change due to the change in true density caused by C converted to SiC. Equation 6 shows the change in diameter when carbon fibers are converted to SiC. From this equation, it can be estimated that the carbon fiber of 7 μm in diameter used in this report changes to the carbon fiber of 8.7 μm after conversion to SiC. As the size change (in diameter) occurs, the stress/strain is caused in the direction of the yarn section (supposed as being a square section. See "Vol% of substance in Si–SiC matrix C/C composites".). It is expressed in Eq. 7.

$$D_2 = D_1 \cdot ((\mathrm{Si}_{28} + \mathrm{C}_{12})/\rho_{\mathrm{SiC}})^{1/3}/(\mathrm{C}_{12}/\rho c)^{1/3} \quad (6)$$

$$\sigma_{\mathrm{c/c}} = E_{\mathrm{c/c}}\,(\Delta L_{\mathrm{c/c}}/L_{\mathrm{c/c}}) \quad (7)$$

Note: Meanings of keys in Eq. 6 and Eq. 7 are shown in Table 2.

Supposing that the tensile strength and the tensile Young's modulus (measured values are included in Table 2) of AC200-C/C composites without Si infiltration are same as those of the yarn surrounded by trunk Si–SiC without Si infiltration, the results of calculation in Eqs. 6 and 7 for the stress causing cracks in yarn and the limited strain (=crack width) are shown in Fig. 14. Supposing that the tensile strength (horizontal axis) varies in the range of the standard deviation of 25.71 around the mean of 61.6 MPa and that the tensile Young's modulus varies in

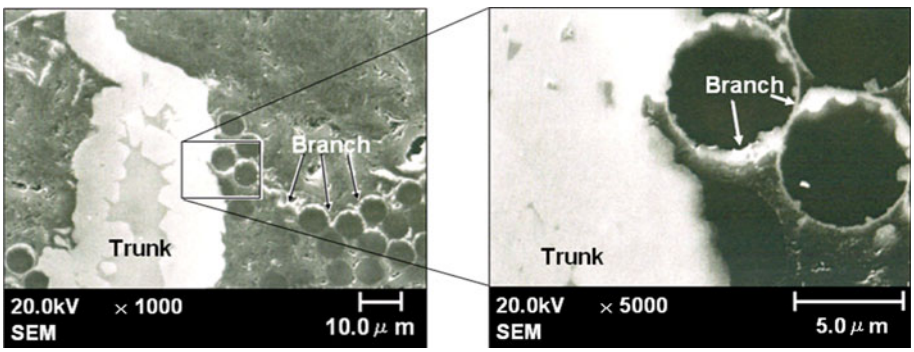


**Fig. 12** Photos of microstructure near Si–SiC matrix. It is the enlarged photo of the area in the upper center of the photo of Sample T3 "Third Step" shown in Fig. 9

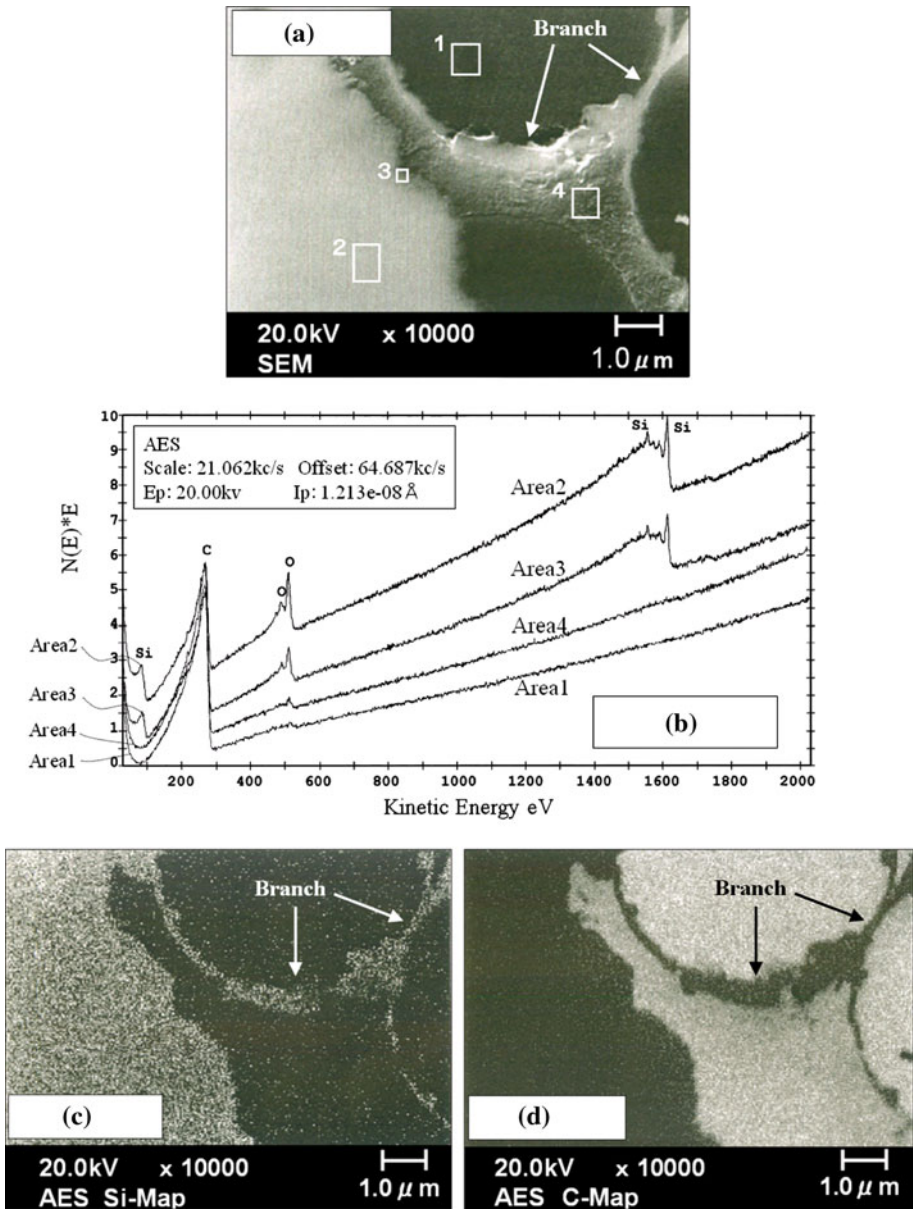


**Fig. 13** Microstructure near Si–SiC matrix (SEM, **a**) and result of Auger analysis (AES, **b–d**). The microstructure of the area in the center in Fig. 12a, the result of Auger Analysis (AES, **b**) in Area 1 to Area 4 and the distribution of Si concentration (**c**) and *C* concentration (**d**) in the SEM area (**a**)

the range of the standard deviation of 21970 around the mean of 50600 MPa, the results were calculated as shown in Fig. 14. According to the results, the crack width (=limit strain) is 0.15–0.92 μm. The values of the crack width agree with the width of branch Si–SiC in the photo of the microstructure in Fig. 13.

## Mechanism of synthesizing dense Si–SiC matrix C/C composites

As mentioned above in Vol% of substance in Si–SiC matrix C/C composites to Trigger for the Third Step of Si–SiC matrix C/C composites synthesis, the mechanism of synthesizing dense Si–SiC matrix C/C composites, where the branch Si–SiC matrix grown from the trunk Si–SiC matrix connects with a bundle of carbon fibers (yarn) tightly, is as follows (Fig. 15):

*First Step*

$SiO/SiO_2$ gas spreads through large pores among yarns at the temperature lower than the Si melting point and SiC films are synthesized in the vapors near the surface of the yarns of low porosity to increase the air tightness on the surface of yarn.

*Second Step*

When the temperature reaches Si melting point and higher, the melted Si infiltrates through the large pores among

**Table 2** Meanings of keys in Eqs. 6 and 7 with data used in this study

| Key | Meaning of key | Data in this study |
|---|---|---|
| $D_1$ | Diameter of carbon fiber | 7.0 μm from Fig. 3 |
| $D_2$ | Diameter of SiC which is converted from carbon fiber | 8.7 μm from Eq. 6 |
| $Si_{28}$ | Atomic weight of Silicon | 28.086 |
| $C_{12}$ | Atomic weight of Carbon | 12.011 |
| $\rho_{SiC}$ | Specific gravity of SiC | 3.15 |
| $\rho_C$ | Specific gravity of C/C composites | 1.9527 (value of AC200-C/C composites) |
| $E_{c/c}$ | Tensile elastic modulus of C/C composites (pre-pregnant sheets layered direction) | Average: 50600 MPa std #: 21970 |
| $\sigma_{c/c}$ | Tensile strength of C/C composites (pre-pregnant sheets layered direction) | Average: 61.6 MPa std #: 25.71 |
| $L_{c/c}$ | Width of yarn in C/C composite | 300 μm from Fig. 3 |
| $\Delta L_{c/c}$ | Strain (=Elongation $(D_2 - D_1)$) | Shown in Fig. 14 |

$E_{c/c}$ and $\sigma_{c/c}$: Measured according to the procedure in Japanese Industrial Standard, JIS R 1606 [25]

std #: Standard deviation by $N = 5$

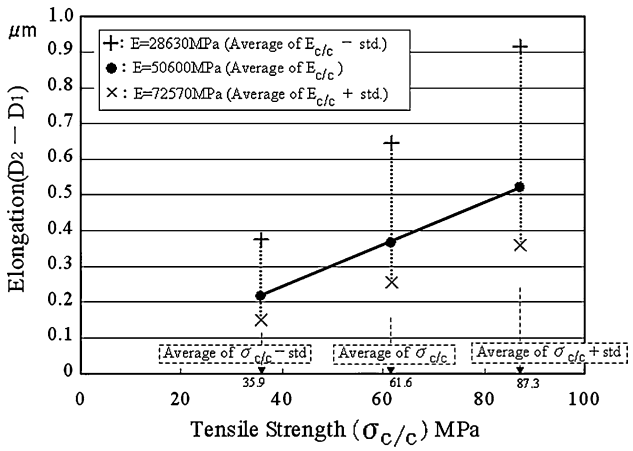


**Fig. 14** Relation between tensile strength and strain in a yarn

yarns and Si reacts with C near the surface of the yarn to synthesize SiC. Then, Si–SiC matrix is formed among yarns. The air tightness at the First Step and the volume expansion caused by SiC synthesis at the Second Step control excess Si infiltration into the inside of the yarn

*Third Step*

As carbon fibers are converted to SiC on the surface of the yarn, volume expansion on the surface of the yarn advances to increase the stress/strain in the yarn. When the stress/

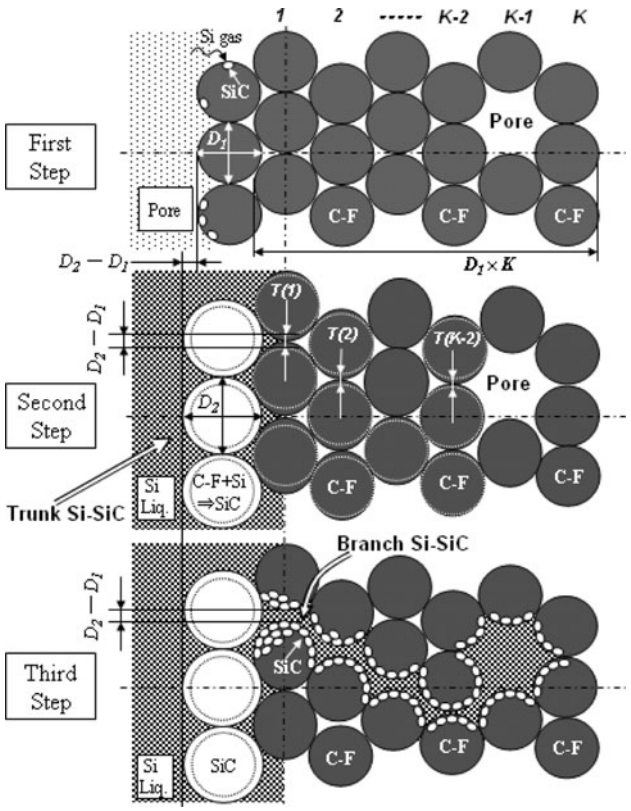


**Fig. 15** Models of synthesis mechanism of Si–SiC matrix C/C composites

strain is higher than the strength of C/C composites, a crack of width corresponding to the stress/strain is generated. Then, Si is re-infiltrated from the trunk Si–SiC matrix at the Second Step to the inside of the yarn through the crack. As the result, the dense Si–SiC matrix C/C composites is synthesized, which has a 3D network where a Si–SiC matrix consisting of trunk Si–SiC and branch Si–SiC connects with the inside of the yarn.

## Conclusion

It is effective in synthesizing dense Si–SiC matrix C/C composites to start with C/C composites (of bimodal pore distribution with large pores among yarns and pores in yarn smaller in diameter than carbon fibers) with 3D-bonded yarns (bundles of dense carbon fibers). After Si infiltration into the C/C composites, there are three steps in synthesizing: "First Step" is to synthesize SiC films on the surfaces of yarns in vapors, "Second Step" is to infiltrate melted Si among yarns for synthesizing SiC films on the yarn surface and thick trunk Si–SiC matrix in the clearances among yarns, and "Third Step" is to synthesize a thin branch Si–SiC matrix through cracks of a new Si-infiltration path in the yarn generated by the stress/strain

due to volume expansion on the yarn surface caused by SiC converted from carbon fibers near the surface of the yarn. As a result, the trunk Si–SiC matrix in the clearances among the yarns and the branch Si–SiC matrix synthesized inside of the yarn, bonds the yarns tightly to create a 3D network for synthesizing a dense Si–SiC matrix C/C composites.

The composites and the procedure in this report are effective industrially because the composites are dense with most carbon fibers un-reacted with Si and because the composites are free from cracks and warps. The structure of the composites obtained approaches the ideal composites proposed by Fitzer. Accordingly, we will continue to study related material properties [26–32].

**Acknowledgements** The author thanks Mr. T. Mizutani, Mr. T. Mizuno and Mr. T. Inaba, Directors of NGK Ins., and Dr. T. Nakagawa, President of Across, for their kind permission to publish this article. The Author also thanks Dr. T. Ohta and Dr. N. Ishizawa, Professors of Nagoya Institute of Technology, and Dr. H. N. Ko, Professor of Nakanihon Automotive College, for their advice in preparation of this article. Lastly, thanks to Mr. Jim V. Castle for proofreading of final document.

## References

1. Popper P (1958) GB-Patent 866813, Application Date: April 8, 1958
2. Weaver JV, Fisher R (1975) US-Patent 4029829, Jan 27
3. Evans CC, Parmee AC, Rainbird RW (1973) GB-Patent 1457757, Nov 28
4. Fitzer E (1987) In: Soumiya S, Moriyoshi Y (eds) SHOUKETSU—case study. Uchida Roukakuho Publishing, Tokyo, p 43
5. Fitzer E, Gadow R (1986) Am Ceram Soc Ceram Bull 65(2):326
6. Chawla KK (2003) Ceramic matrix composites. Kluwer Academic Publishers, Boston
7. Rossignol JY, Quenisset JM, Hannache H, Mallet C, Naslain R, Christin F (1987) J Mater Sci 22:3240. doi:10.1007/BF01161188
8. Zheng GB, Sano H, Uchiyama Y, Kobayashi K, Cheng HM (1999) J Mater Sci 34:p827. doi:10.1023/A:1004589316992
9. Naslain R, Guette A, Rebillat F, Le Gallet S, Lamouroux F, Filipuzzi L, Louchet C (2004) J Mater Sci 39:7303. doi:10.1023/B:JMSC.0000048745.18938.d5
10. Dezellus O, Jacques S, Hodaj F, Eustathopoulos N (2005) J Mater Sci 40:2307. doi:10.1007/s10853-005-1950-7
11. de Omena Pina SR, Yoshida IVP, Pardini LC (2007) J Mater Sci 42:4245. doi:10.1007/s10853-006-0688-1
12. Ouyang H, Li H, Qi L, Li Z, Fang T, Wei J (2008) J Mater Sci 43:4618. doi:10.1007/s10853-008-2664-4
13. Chang T, Nakagawa T, Okura (1991) A studies on a new manufacturing process of carbon fiber reinforced carbon matrix (C/C) composites, Report of the Institute of Industrial Science, Tokyo University, vol 35, No. 8, Serial No. 229 Feb [in Japanese]
14. http://www.across-cc.co.jp/jp/index.html
15. http://www.materials.elkem.com/
16. Hanzawa S, Komiyama T (1997) JP-Patent 2642561
17. Kanai H, Sugihara S, Yamaguchi H, Uchimura T, Obata N, Kikuchi T, Kimura F, Ichinokura M (2007) J Mater Sci 42:9529. doi:10.1007/s10853-007-2090-z
18. Li JG, Hausner H (1991) J Mater Sci Lett 10:1275
19. Hanzawa S, Nakagawa T (2003) JP-Patent 3491902
20. Gern FH, Kochendörfer R (1997) Composites Part A 28:355
21. Janaf thermochemical tables (1985) J Phys Chem Ref Data, vol 14, Suppl 1, pp 535, 536, 626, 628, 633, 634, 1650, 1667, 1673, 1765, 1678, 1796, 1767, 1799
22. Goto T, Narushima T, Iguchi Y, Hirai T (1994) In: Nickel KG (ed) Corrosion of advanced ceramics, vol 267. Kluwer Academic Publishers, the Netherlands, p 165
23. Hanzawa S (2010) Refractory of furnace to reduce environmental impact, Annual Report of the Ceramics Research Laboratory, Nagoya Institute of Technology, vol IX, pp 33–42 [in Japanese]
24. Aiba Y, Usami Y (1973) JP-Patent application S54-99615
25. JIS R-1606 (2000) Testing methods for tensile strength of fine ceramics at room and elevated temperature, Revised 1995-04-01
26. Hanzawa S, Nakano K (1999) Ceram Soc Jpn 34(6):431
27. Matsubara T, Takao Y, Wang WX, Hanzawa S (2000) In: Proceedings of the second Asia-Australasian conference on composite materials (ACCM-2000), Kyongju, Korea, vol 2, pp 701–706, 2000.08
28. Ogasawara T, Ishikawa T, Matsuzaki T, Hanzawa S, Kato R (2000) In: Proceedings of the 22nd international symposium on space technology and science, ISTS2000-c-23, Morioka Japan, 2000.05
29. Ogasawara T, Ishikawa T (2001) J Am Ceram Soc 84(7):1559
30. Wang WX, Iihoshi K, Matsubara T, Takao Y (2001) In: Proceedings of the ICCM-13, Beijing, CDROM ID-1432, pp 1–8, 2001.01
31. Moriyama M, Takao Y, Wang WX, Matsubara T (2004) In: Proceedings of the 11th US-Japan conference on composite materials, pp C/C2.1–2.4, 2004.09
32. Moriyama M, Takao Y, Wang WX, Matsubara T (2010) Int J Fatigue 32:208